Effect of Reynolds Number on Upper Cowl Flow Separation

Werner Hoelmer* and James L. Younghans†
General Electric Company, Cincinnati, Ohio
and
Jean Claude Raynal‡
ONERA, LeFauga-Mauzac, France

This paper describes testing on subsonic inlet cowlings for high-bypass-ratio turbofan engines, conducted in a low-speed pressurized wind tunnel. These new data bridge the gap between earlier low Reynolds number model data for cowl flow separation and full-scale flight conditions. Innovative model test approaches were employed and are described. New cowl flow separation data matched previously obtained data at comparable Reynolds numbers. Higher Reynolds number data, up to flight value levels, behaved in an orderly fashion and were suitable for improving currently available theroretical descriptions of the phenomena governing engine inoperative cowl flow separation.

Nomenclature

H = shape factor
K = surface curvature
MFR = mass flow ratio
P = pressure
R = radius
Re = Reynolds number
S = surface distance
U = velocity
Z = distance normal to surface
α = angle of attack
δ^* = displacement thickness
Θ = momentum thickness
θ = surface angle

Subscripts

DHL = hilite diameter
E = engine face
HL = hilite
INLET = inlet
L = local
MAX = maximum
P = peak
SEP = separation
T = total, stagnation
TH = throat
0 = freestream
1 = S/DHL = 0.009
2 = S/DHL = 0.060

Introduction

AERODYNAMIC design conditions for high-bypass-ratio commercial transport aircraft nacelles are typically the low-speed takeoff and landing conditions as well as the high-speed cruise conditions. The low-speed design condition involves both the requirement for high-angle-of-attack operation during takeoff (Fig. 1) as well as the potential for low mass flow ratio associated with an inoperative engine. The lower inlet lip aerodynamic shape is usually determined by the high-flow, high-angle-of-attack condition that has been shown to be relatively insensitive to Reynolds number,[1] while the upper external cowl shape has been determined to be Reynolds number dependent. The upper inlet external cowl is simultaneously exposed to conditions of high angle of attack and low mass flow in the event of an inoperative engine burning second segment climb after takeoff. This creates a region of high surface Mach number that, if not carefully considered during the aerodynamic design phase, can lead to cowl flow separation downstream of the inlet lip leading edge. This flow separation can cause an aircraft drag increase that is on the order of 3–5% of total aircraft drag. If the aircraft is thrust limited during this flight segment, which is usually the case for two- and three-engine aircraft, the engine thrust must be increased and the vertical tail size may also require upward sizing. Even in the case of a four-engine aircraft, where thrust is not as critical, an inoperative engine during second-segment climb can cause external cowl separation, which induces aircraft buffetting that might be misinterpreted as wing buffetting. This is undesirable for flight safety considerations. Therefore, the nacelle designer is charged with producing an external cowl upper lip shape that does not separate while operating within the aircraft flight placard (Fig. 2). The effect of cowl flow separation on the onset of wing stall is not considered here because the objective, as stated, is to design a cowl shape that will not separate prior to the onset of wing stall.

The nacelle designer must usually make design judgments based on subscale Reynolds number testing, even when pressurized wind tunnel facilities such as LeFauga[2] are available, since full-scale model simulation is not generally feasible due to size or cost limitations. The question of how to extrapolate these results to full scale is a critical one for the designer. Utilizing the subscale results per se can result in a nacelle diameter and weight penalty, as well as an isolated and installed drag penalty. To avoid such penalties, the designer must have criteria for extrapolating the subscale results to full scale. A supplemental test program was, therefore, conducted by General Electric at LeFauga in late 1982 to assess the subscale Reynolds number question. The 15% scale model data obtained in 1981 were augmented by 33% scale model date to provide full-scale Reynolds number simulation for the external cowl with engine-inoperative simulation. Due to the facility's piping limitations, full-scale Reynolds number data

Received April 11, 1985; revision received Dec. 2, 1985.

*Program Manager, Aviation Service Department, Aircraft Engine Business Group. Member AIAA.
†Manager, Low Observables Systems Evaluation and Integration, Aircraft Engine Business Group. Associate Fellow AIAA.
‡Test Engineer.

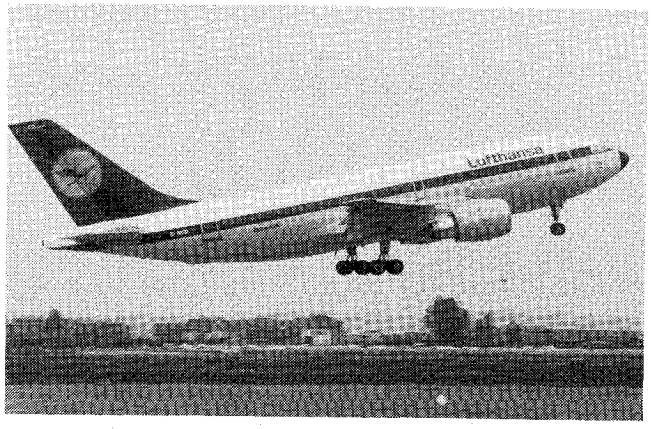

Fig. 1 Typical aircraft incidence during takeoff.

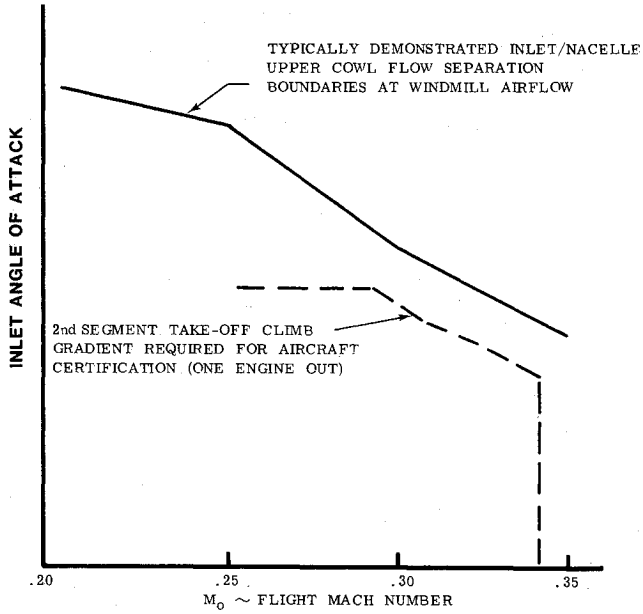

Fig. 2 Typical nacelle external flow separation boundaries for second-segment takeoff climb.

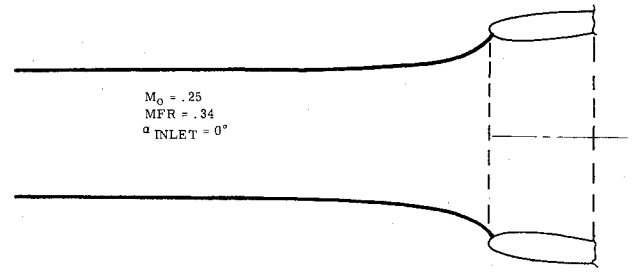

Fig. 3 Inlet flowfield for windmill condition at zero angle of attack.

for the lower lip operability testing could not be obtained for the 33% scale model. It should be noted that the larger model size was selected to permit some overlap with the 15% scale model test results as well as full-scale Reynolds number simulation. A further objective of the 33% scale model testing was to obtain sufficiently detailed data to further advance understanding of the separation phenomenon.

The Aerodynamic Problem

When an engine is inoperative (windmilling) during initial climb, flow separation on the upper cowl surface can cause an unacceptable drag increase, preventing the aircraft from meeting prescribed climb gradients. The conditions governing the onset of this type of flow separation must be determined and understood, in order to develop inlet (cowl) designs that exhibit attached flow within the aircraft operating envelope.

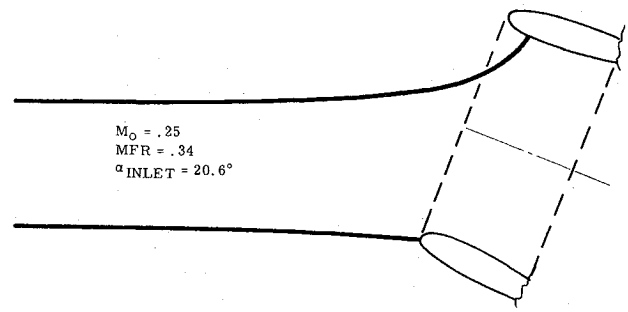

Fig. 4 Inlet flowfield for windmill condition near separation angle of attack.

Mass flow ratios associated with a windmilling turbofan engine are typically in the 30–35% range. The capture stream tube and associated stagnation streamlines that characterize the nacelle flowfield during the windmilling condition are shown schematically in Figs. 3 and 4 for 0 and 20 deg angle of attack, respectively. Figure 4 depicts the inlet flowfield near the external flow separation. Specifically, the stagnation point at the top vertical centerline lies well inside the internal lip. The external flow, originating at the stagnation point, moves forward toward the hilite, accelerating to transonic velocities on the inlet external surface immediately downstream of the hilite. The flow then decelerates to near-freestream velocities farther down the inlet cowl. Associated boundary-layer development is laminar near the stagnation point and then, if the freestream Reynolds number is sufficiently high, may transition before reaching the hilite. Downstream of the hilite, where the suction peak occurs, the onset of massive separation/stall at the critical inlet angle of attack can be caused by 1) laminar separation bubble bursting, 2) turbulent boundary-layer separation, or 3) a combination of the two phenomena.

For a number of years, laminar separation bubble bursting has been studied in conjunction with wing and cascade leading-edge stall. Roberts[3] has developed a semi-empirical technique for the description and calculation of the development and bursting of laminar separation bubbles in airfoil sections. He postulates that, if the surface of the airfoil is smooth and the freestream turbulence low, the laminar boundary-layer can separate due to the pressure gradient aft of the velocity peak. Transition occurs in the separated shear layer and the flow reattaches to the airfoil surface as a turbulent boundary layer. This flow phenomenon is termed a short laminar separation bubble (Fig. 5). A sufficient increase in the angle of attack can cause the turbulent free shear layer to fail to reattach. According to Roberts,[3] this is short bubble bursting and is the cause of abrupt/massive leading-edge stall.

When the freestream Reynolds number based on the airfoil chord length is sufficiently high (greater than 3×10^6) and the airfoil nose is sufficiently blunt, then, according to Van Den Berg,[4] turbulent boundary-layer separation is the cause of leading-edge stalls. Therefore, external separations for the test conditions presented in this paper are not a result of laminar bubble bursting, but rather are of turbulent boundary-layer separation.

Although the foregoing suggests a general understanding of the flow behavior near the leading edge of airfoils and three-dimensional inlets at the onset of external flow separation, theoretical calculations of these aerodynamically complicated processes are not sufficiently advanced to permit application to general three-dimensional inlets. Thus, the inlet/nacelle designer relies heavily on separation boundaries determined in subscale model tests. As new and more detailed data are taken, it will be possible to develop semi-empirical techniques

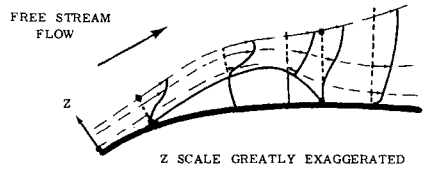

Fig. 5 Schematic of laminar separation concept.

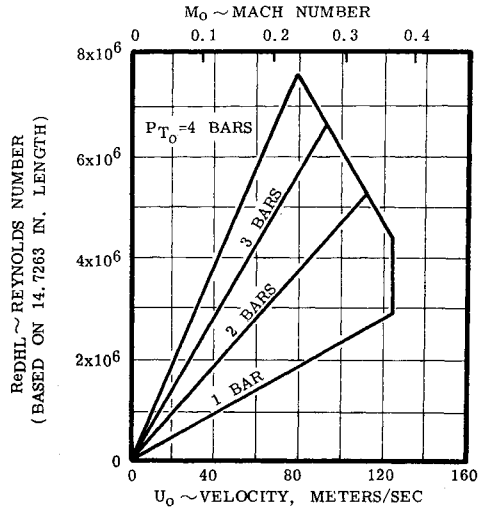

Fig. 6 LeFauga Mach number/Reynolds number envelope.

and to modify the computational algorithms suited for predicting separation in three-dimensional external (internal) inlet flowfields.

Subscale Model Tests

Facility

All testing described herein was conducted at the ONERA Centre LeFauga-Mauzac.[2] The variable desity F1 tunnel has a 4.5×3.5 m test section with a maximum velocity of 120 m/s and a stagnation pressure that can be varied between 1.0 and 4.0 bars. The stagnation pressure variability is Mach-number dependent, as indicated in Fig. 6.

Specific features that made this facility attractive for the external flow separation studies were the Reynolds number ranges achievable, the continuous sweep of the angle-of-attack mechanism, and the on-line data acquisition/reduction capabilities.

15% Scale Model Test

Inlet/nacelle development testing conducted by the General Electric Company at LeFauga in 1981 included a 15% scale model of an axisymmetric inlet geometry (Fig. 7a). Geometric details of the lip region are shown in Fig. 7b. The photograph of the model (Fig. 8) identifies a set of external total pressure rakes used for detecting the onset of separation. The rakes did not affect the onset of separation because of their design and location. Subsequent testing without these rakes produced identical lip separation behavior. Instrumentation also included limited wall static pressures in the lip region.

An example of how both types of instrumentation identified external flow separation is given in Fig. 9. Note, that both the lip wall static pressure and the external rake total pressure indicate the same value of flow separation angle, substantiating massive separation over the entire upper cowl surface.

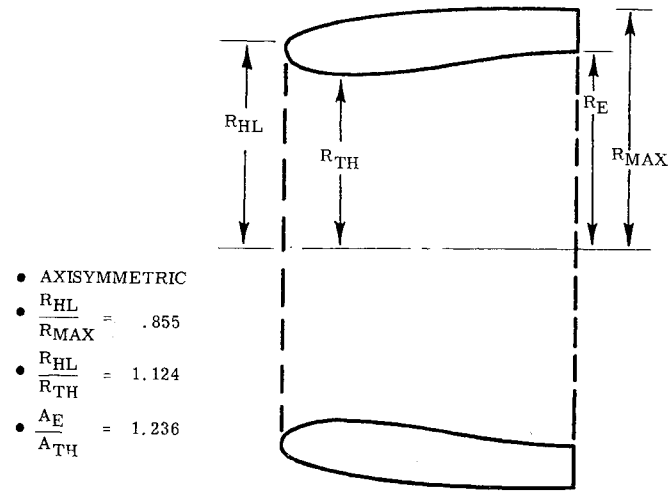

Fig. 7a 15% scale model geometry schematic.

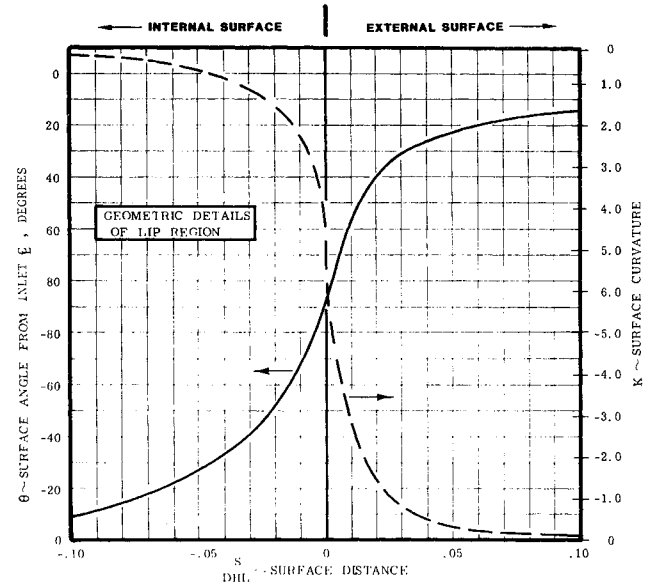

Fig. 7b 15% scale model lip geometry details.

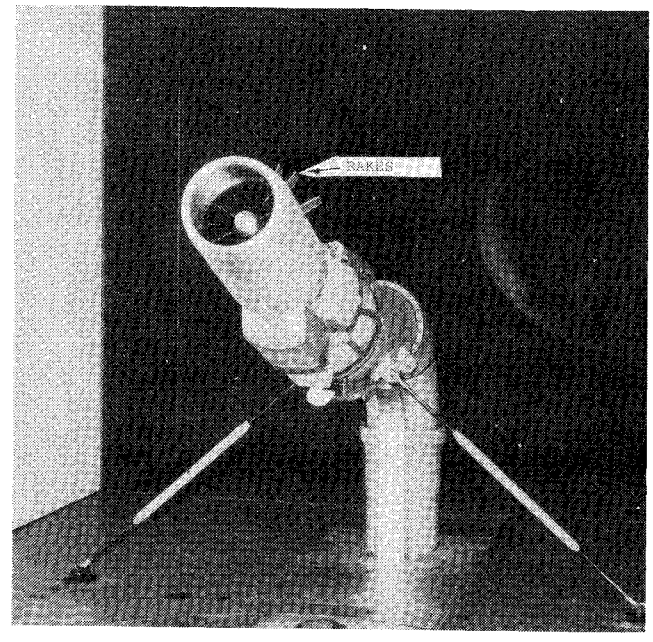

Fig. 8 15% scale model at LeFauga.

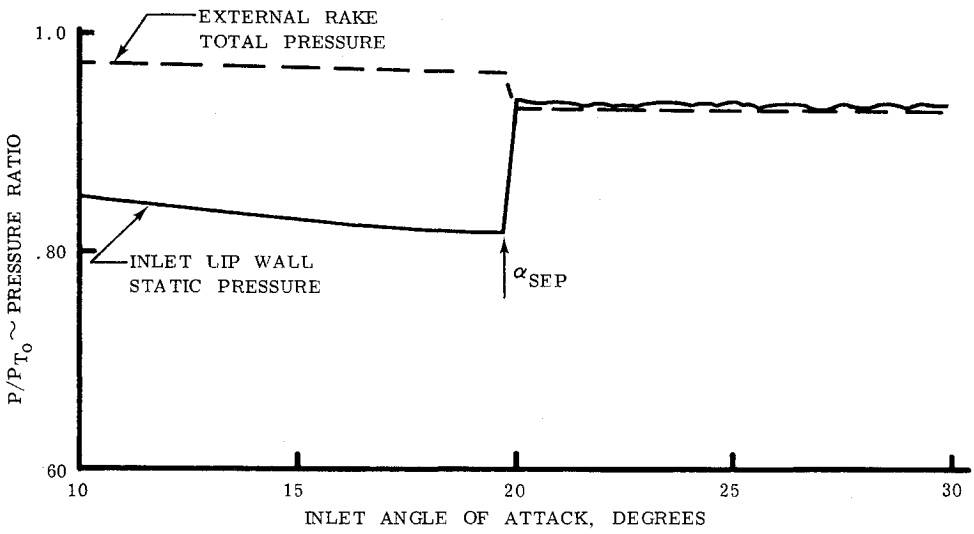

Fig. 9 Experimental technique for determining external flow separation.

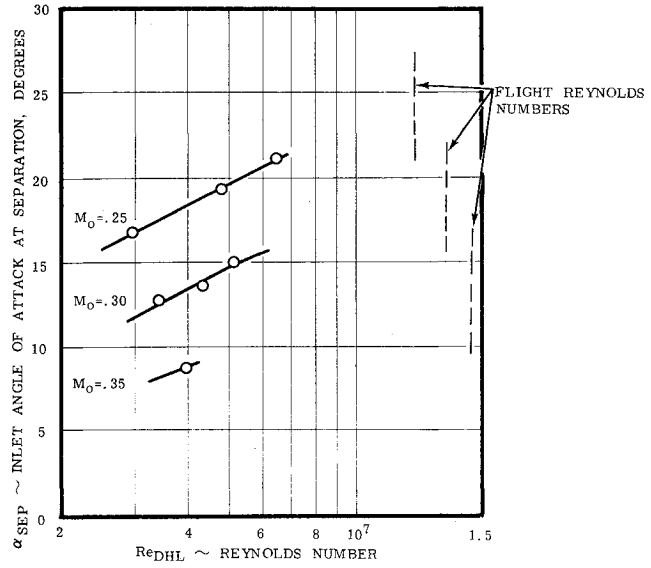

Fig. 10 External flow separation data for 15% scale model.

Separation boundaries were established for a range of freestream Mach numbers and Reynolds numbers (Fig. 10). Strong Reynolds number dependence is exhibited. This same level of dependence has been witnessed before for other inlet designs[1] and was expected. The question of how to extrapolate these results to full scale is critical. When the analytical techniques available in 1981 failed to provide a clear understanding of the Reynolds number trends exhibited by the 15% scale model data, it was decided to develop experimental means to bridge the gap between the 1981 data base and full-scale flight.

33% Scale Model Test

The concept of testing a large inlet model at LeFauga was prompted by the need to fill the Reynolds number gap in the data base. As shown in Fig. 11, the 33% scale model can attain full-scale Reynolds number data at both Mach 0.20 and M 0.25 conditions. Other considerations affecting the decisions were, of course, flow system capability, model cost, model construction difficulties, and, finally, the ability to operate this large model (with its attendent large aerodynamic loads) on the existing 15% scale model support system.

The mechanical problems were overcome with significant help from ONERA. The model test was conducted in late 1982. Figure 12 illustrates the technique ONERA devised to counterbalance the large aerodynamic loads at the angle of attack. Note the cable that stretches from the model lower surface through the test section floor. The cable can also be seen in the photographs of the 33% scale model (Fig. 13). The mechanical arrangement worked as designed and permitted the gathering of separation data over the complete range of the test variables.

To increase the aerodynamic information and, ultimately, understand the flow phenomena governing external cowl flow separation, the test techniques were modified. The first change was to add additional static pressure taps in the lip region. The second was to eliminate the external total pressure rakes. Since the lip wall static pressures and rake total pressures had consistently given identical values of the flow separation angle, it was felt that the redundancy could be removed from the test.

Finally, a change in procedure permitted continuous sampling of key lip wall static pressures so the variation of the Mach number distribution during a sweep could be recorded. This provided substantially more insight into the lip aerodynamics leading up to and including external flow separation. A sample of how the lip Mach number data were then reduced on-line is shown in Fig. 14. Note how all pressure tap locations, external and internal, indicate the separation phenomenon at exactly the same inlet angle of attack. The sweep rate was generally about 1 deg/s, essentially steady state, but could be changed if desired. Data were obtained with steady-state, close-coupled transducers.

A summary of the external flow separation data for the 33% scale model is shown in Fig. 15. The data are well behaved. They show Mach number dependence similar to the 15% scale model data, but lose Reynolds number dependence as they approach a Reynolds number of 10×10^6 (based on model hilite diameter). Figure 16 combines both the 15 and 33% scale model data. A good match of these two sets of data is exhibited. The data fill the gap between the small-scale data and full-scale Reynolds numbers. The characteristics of each Mach number curve should be suitable for extrapolating other subscale data to full-scale Reynolds numbers.

Data Correlation and Analysis

The well-behaved, detailed lip Mach number data obtained during the 33% scale model test provided a data base for simple correlation studies and comparisons with available basic inviscid/viscous flow analyses.

Analyses currently employed by the General Electric Company for designing/evaluating three-dimensional inlet/nacelle configurations are described in Refs. 5–7. These analytical techniques properly handle inviscid, compressible, three-dimensional flowfields as well as boundary-layer development

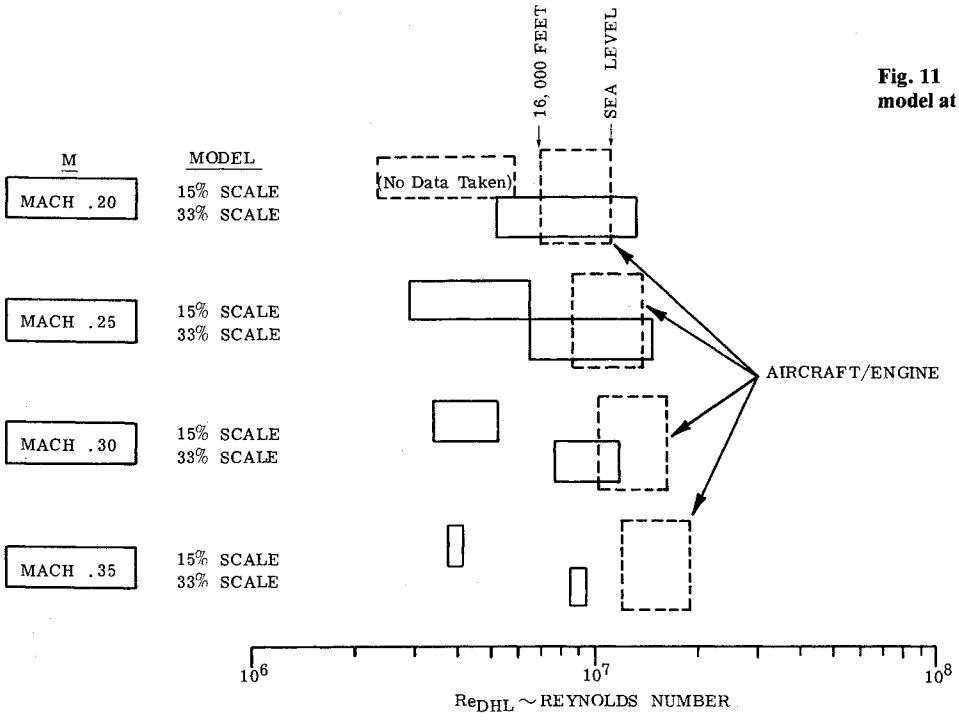

Fig. 11 Reynolds number envelope for 33% scale model at LeFauga.

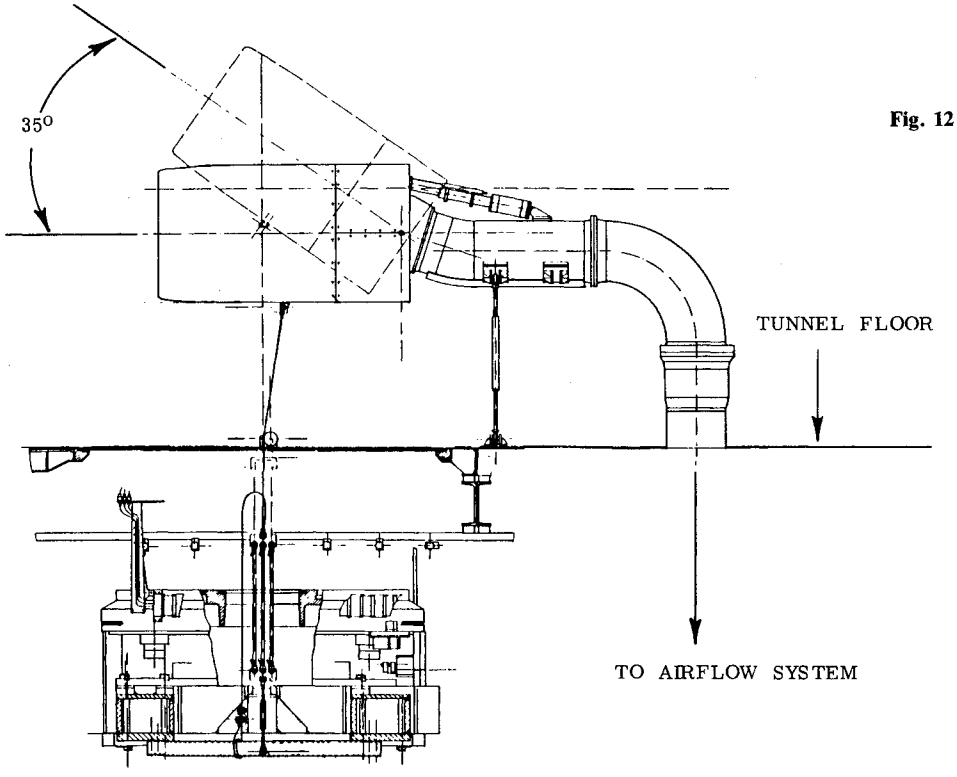

Fig. 12 33% scale model installation schematic.

in the absence of shocks and separation. When the onset of flow separation is coupled with the formation of a three-dimensional laminar separation bubble, for instance, a semi-empirical technique such as proposed by Roberts[3] would be needed to achieve a complete theoretical solution. If the flow separation is due to turbulent boundary-layer separation alone, then correlation and analytical techniques currently available may be suitable.

Data obtained for the 33% scale model, although more detailed than the 15% scale model data, were not adequate to define the onset of a very short laminar bubble or any of the upstream or downstream laminar/transitional/turbulent boundary-layer characteristics. The primary purpose of the tests described herein was to obtain external flow separation boundaries at full-scale Reynolds number. Although many flow details were not obtained, the wall Mach number data provided a basis for assessing certain basic analyses as well as permitting data correlations.

Wall Mach number data in the lip region were compared to the inviscid theory of Ref. 6 for three inlet angles of attack of 0–20.6 deg (Fig. 17). Excellent agreement with the inviscid theory was obtained everywhere except for a relatively small

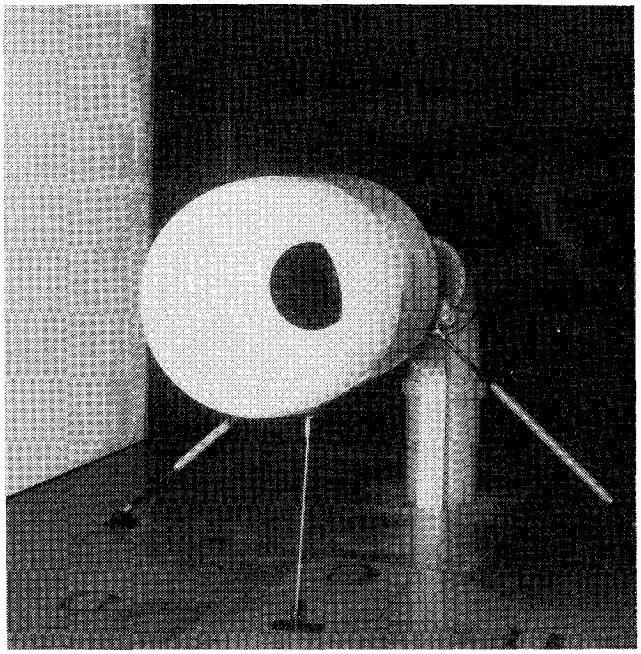

Fig. 13 33% scale model at LeFauga.

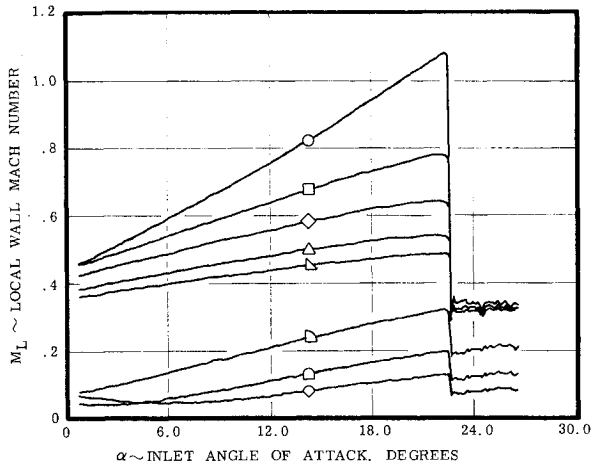

Fig. 14 Improved wall Mach number data acquisition technique.

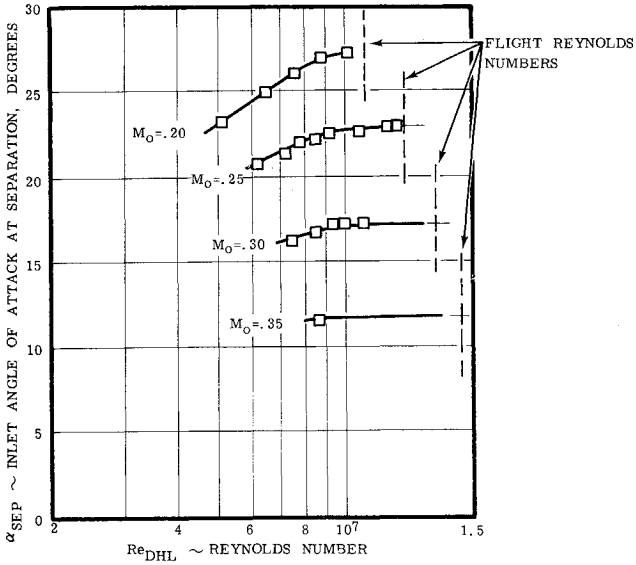

Fig. 15 External flow separation data for 33% scale model.

discrepancy near the peak Mach number point. The theoretical value of 1.00 was somewhat lower than the experimental value of 1.05. This may be considered acceptable, since viscous effects, such as boundary-layer displacement thickness, were not taken into account. It should be noted that the 20.6-deg data were taken 0.1 deg prior to flow separation.

To further understand how well the inviscid theory is able to predict the peak Mach number from zero angle of attack to the angle of attack at separation, two sets of data were compared with the inviscid theory. Results of this comparison are shown in Fig. 18. Theory and data differences are small at low values of inlet angle of attack for both sets of Reynolds number data, but the differences start to increase at higher values. At separation, the difference between theoretical and experimental Mach numbers is 0.05 for the lower Reynolds number data and 0.11 for the higher values.

A correlation of the ratio of peak wall Mach number to downstream Mach number (S/DHL = 0.06), with both freestream Mach number and Reynolds number, was attempted to test whether the external Mach number gradient prior to separation behaved in an orderly manner. Figure 19 shows the result of data correlated at incipient flow separation conditions. The data show distinct Mach number and Reynolds number dependence. Note the expanded vertical scale that shows all of the data to fall between the wall Mach number gradient values of 2.09 and 2.33.

Since the external Mach number gradient correlation of Fig. 19 looked promising, a similar type of correlation using the ratio between the velocity at a model station just downstream of the hilite (S/DHL = 0.009) and the freestream velocity was tried. For the same data points as in Fig. 19, the velocity gradient correlation tended to mask the Mach and Reynolds number effects (Fig. 20). Scatter in the data generally fell within ±1% of the mean value of 3.70. The scatter represents uncertainty in angle of attack of ±0.5 deg for a Mach 0.25, 6.3×10^6 Reynolds number case. This correlation is excellent considering the ranges of Reynolds numbers, Mach numbers, mass flow ratios, and angles of attack.

An attempt was also made to begin the key analysis of viscous flow from the internal stagnation point to eventual transitional/turbulent boundary-layer separation downstream of the suction peak. To obtain the basic viscous solution, the inviscid pressure distribution from Ref. 6 was combined with the Harris-Blanchard[7] boundary-layer program. The computer program of Ref. 7 solves compressible laminar, transitional, or turbulent boundary-layer equations for two-dimensional or axisymmetric perfect gas flows. A key input to

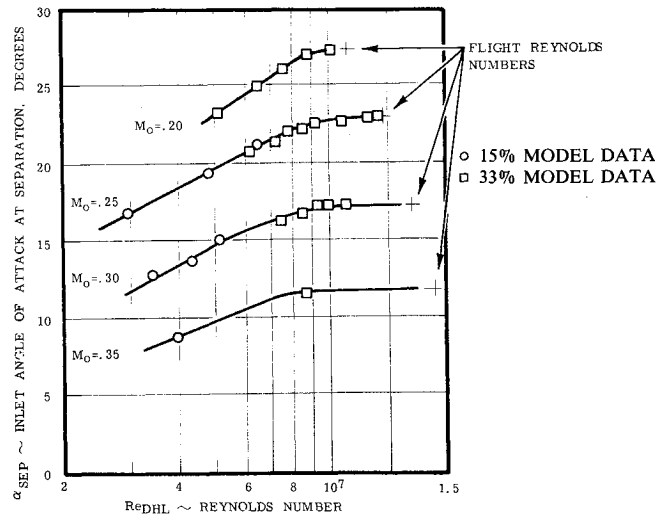

Fig. 16 External flow separation data summary.

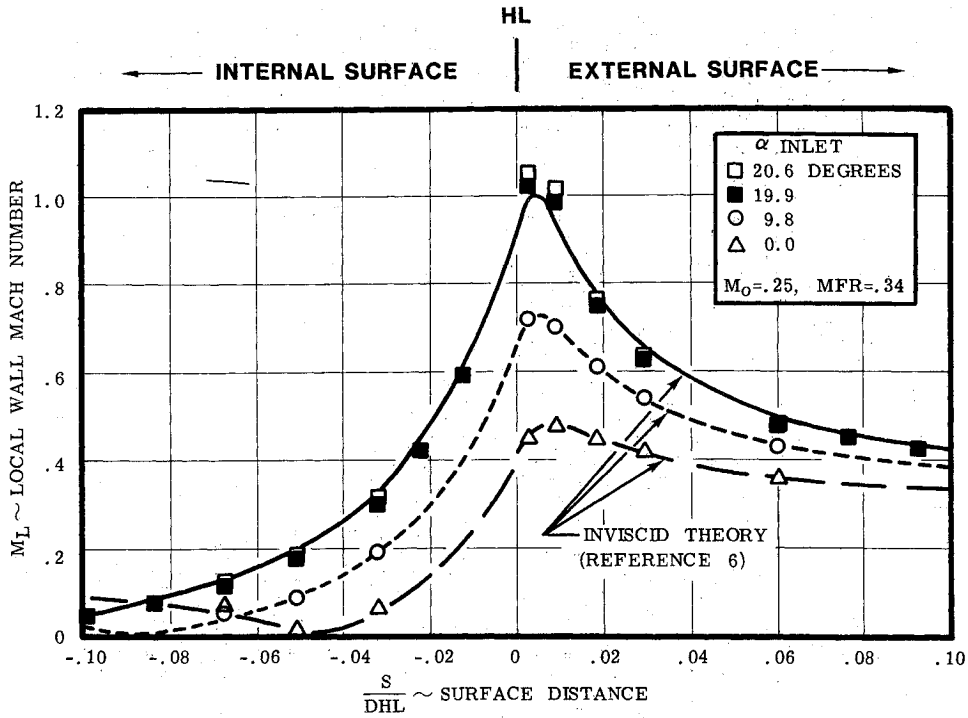

Fig. 17 Inviscid theory/wall Mach number data comparison.

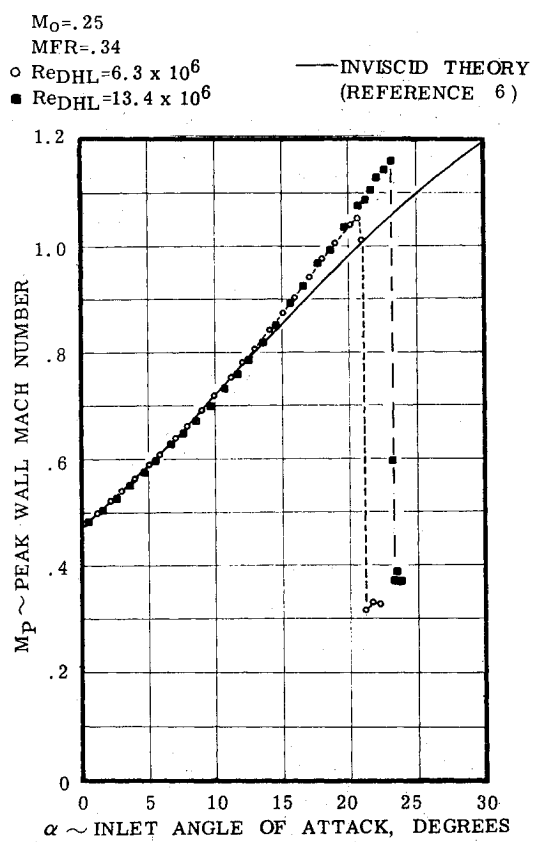

Fig. 18 Comparison of peak wall Mach number prediction with data.

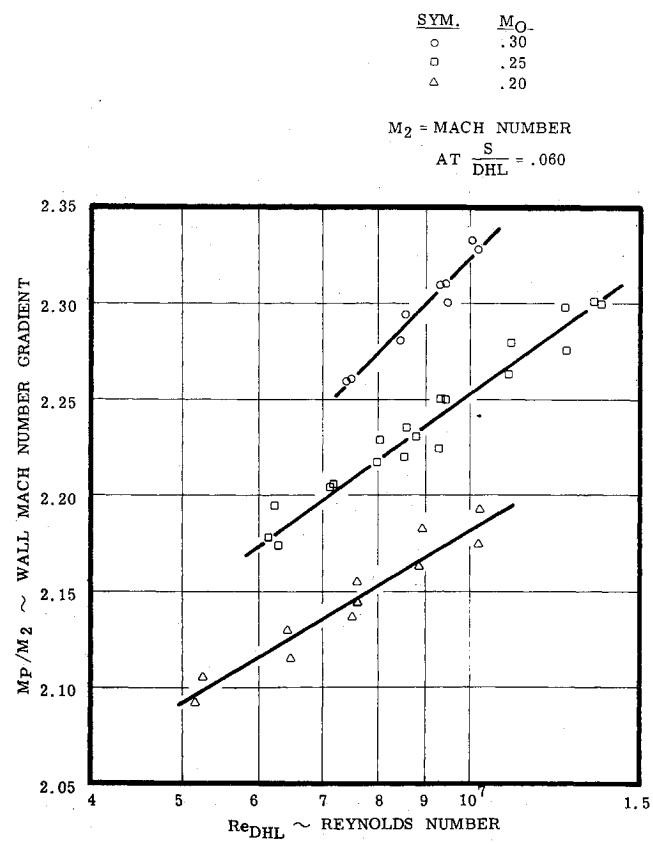

Fig. 19 Wall Mach number gradient data at external flow separation conditions.

the program solution is the location of boundary-layer transition. For the geometry and flow conditions of this study, the guideline of using a momentum thickness Reynolds number equal to 140 was used.[4]

A sample calculation using this transition criterion for the 20.6 deg 6.3×10^6 Reynolds number test case was performed. Values of key boundary-layer parameters in the lip region are shown in Fig. 21. Both displacement thickness and momentum thickness grow rapidly aft of the hilite, suggesting that displacement thickness correction to the inviscid surface shape must be made when close agreement between theory and data is needed. This test case did not predict turbulent boundary-layer separation. Solutions were then obtained at this Reynolds number for increasing values of inlet angle of attack. Separation was predicted for $\alpha = 24.0$ deg, 3.4 deg higher than the value indicated by the 33% model data. A similar ex-

ercise for the higher Reynolds number condition resulted in a 5.4 deg overprediction. A key reason for this disagreement is the underprediction of the external pressure (Mach number) gradient (see Figs. 17 and 18). This underprediction may be due to inadequate compressibility corrections in the analysis[6] and/or a need to correct the inviscid surface for the boundary-layer displacement thickness. Predicted separation angles agreed much better with the data when experimental pressure distributions were used (Fig. 22).

Substantial progress has been made in understanding/predicting the external flow separation characteristics of the 33% scale model of this study. Techniques and procedures developed (Figs. 19 and 20) should be qualitatively applicable to other inlet/nacelle geometries. Quantitative application would require verification via additional inlet data correlation.

Future effort will be directed toward improving inviscid/viscous analytical techniques and checking correlations with existing data for both axisymmetric and three-dimensional inlets. This should provide a design tool for predicting external cowl flow separation.

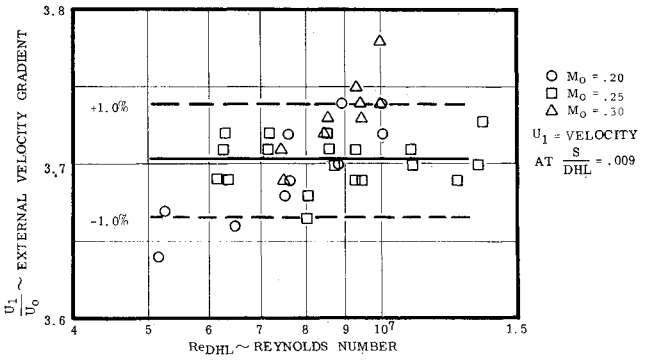

Fig. 20 Velocity gradient data at external flow separation conditions.

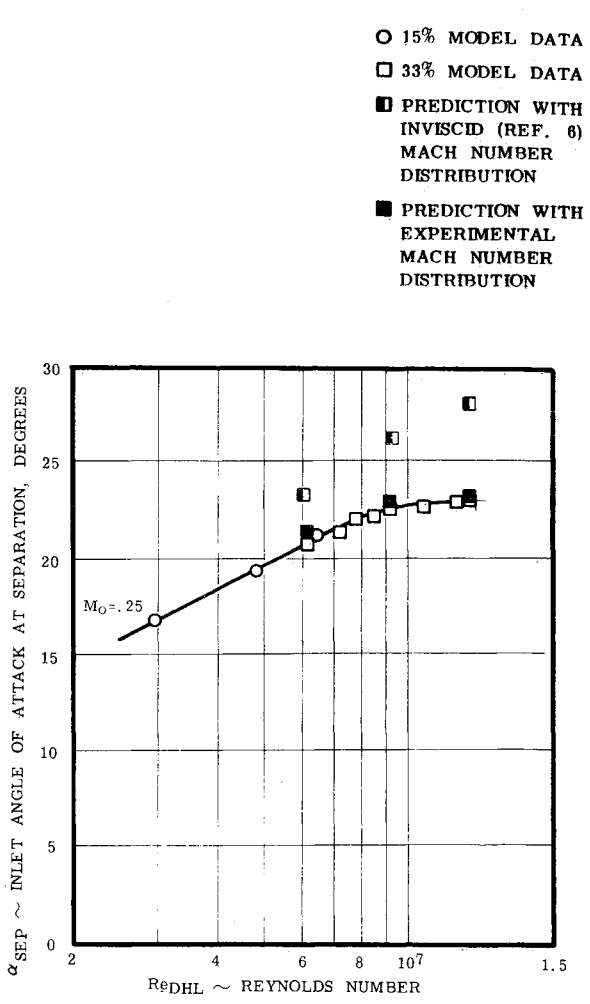

Fig. 22 Comparison of turbulent boundary-layer separation prediction with data.

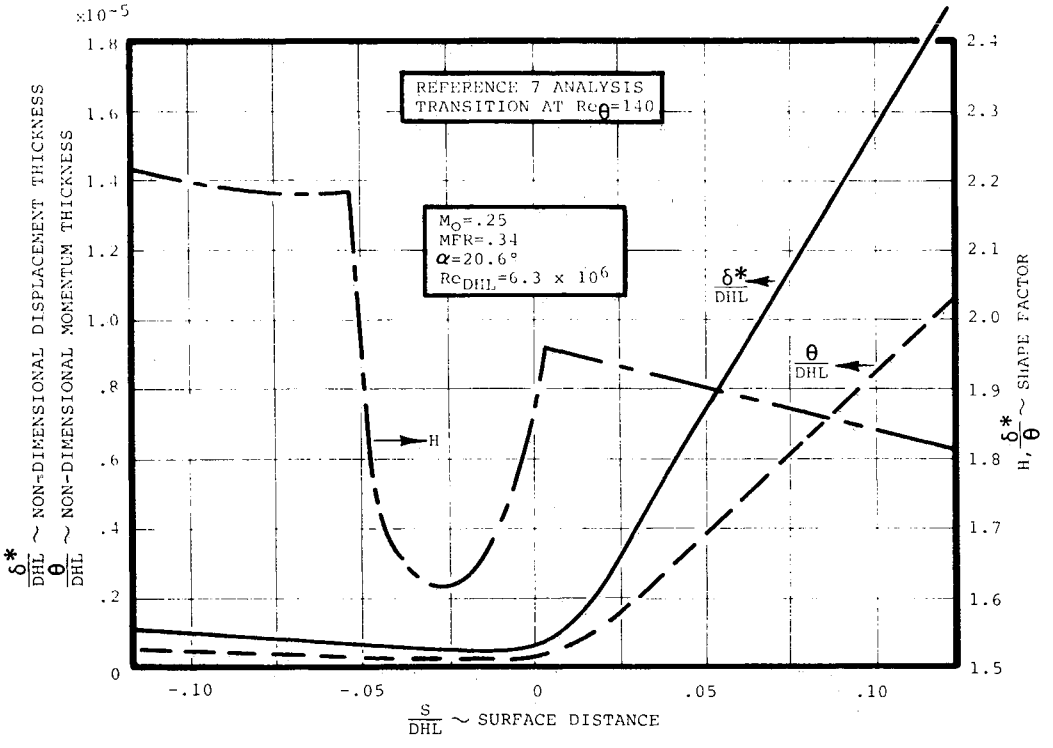

Fig. 21 Typical values of boundary-layer parameters in lip region near external flow separation.

Conclusions

1) Flight Reynolds number dependence of upper cowl flow separation has been experimentally determined by testing a 33% scale inlet model in a pressurized low-speed tunnel.

2) The data exhibited orderly behavior, matched with previously obtained 15% scale inlet model data, and trends are suitable for extrapolating other small-scale data to flight Reynolds numbers.

3) New test techniques generated detailed lip Mach number distributions at inlet angles of attack leading to external flow separation.

4) Analysis of detailed inlet lip data suggests that turbulent boundary-layer separation is the probable cause of external flow separation for the lip geometry and Reynolds number range of this study.

Acknowledgments

The authors wish to express their gratitude to the following individuals and organizations who contributed greatly to either the test program and/or the subsequent analyses: Mr. A. Lingen, General Electric Program Sponsor; Mr. J. P. Ledy, ONERA Program Director; Mr. A. G. Fine, General Electric Aerodynamic Test Engineer; and Mr. N. O. Stockman, General Electric Computer Specialist.

References

[1]Younghans, J. L., Hoelmer, W., and Stockman, N. O., "Low Speed Effects of Reynolds number and Lip Geometry on High Bypass Ratio Inlet Performance," AIAA Paper 82-0059, Jan. 1982.

[2]Carrara, M. M. and Masson, A., "Three Years of Operation of the ONERA Pressurized Subsonic Wind Tunnel," ONERA Tech. Paper 1980-129, Oct. 1980.

[3]Roberts, W. B., "Calculation of Laminar Separation Bubbles and Their Effect on Airfoil Performance," *AIAA Journal,* Vol. 18, Jan. 1980, pp. 25-31.

[4]Van Den Berg, B., "Role of Laminar Separation Bubbles in Airfoil Leading-Edge Stalls," *AIAA Journal,* Vol. 19, May 1981, pp. 553-556.

[5]Lahti, D. J., Dietrich, D. A., Stockman, N. O., and Faust, G. K., "Application of Computational Methods to the Design of Large Turbofan Engine Nacelles," AIAA Paper 84-0121, Jan. 1984.

[6]Stockman, N. O. and Farrel, C. A. Jr., "Improved Computer Programs for Calculating Potential Flow in Propulsion System Inlets," NASA TM-73728, 1977.

[7]Harris, J. E. and Blanchar, D. K., "Computer Program for Solving Laminar, Transitional, or Turbulent Compressible Boundary-Layer Equations for Two-Dimensional and Axi-Symmetric Flow," NASA TM-83207, 1982.